

Neurological Deficits of an *Rps19*(Arg67del) Model of Diamond-Blackfan Anaemia

(Diamond-Blackfan anaemia / RPS19 / transgenic mouse / gait / neuromuscular function / fear conditioning)

A. KUBIK-ZAHORODNA, B. SCHUSTER, I. KANCHEV, R. SEDLÁČEK

Laboratory of Transgenic Models of Diseases, Division BIOCEV, Institute of Molecular Genetics of the ASCR, v. v. i., Prague, Czech Republic

Abstract. Diamond-Blackfan anaemia is a rare disease caused by insufficient expression of ribosomal proteins and is characterized by erythroid hypoplasia often accompanied by growth retardation, congenital craniofacial and limb abnormalities. In addition, Diamond-Blackfan anaemia patients also exhibit a number of behavioural abnormalities. In this study we describe the behavioural effects observed in a new mouse mutant carrying a targeted single amino acid deletion in the ribosomal protein RPS19. This mutant, created by the deletion of arginine 67 in RPS19, exhibits craniofacial, skeletal, and brain abnormalities, accompanied by various neurobehavioural malfunctions. A battery of behavioural tests revealed a moderate cognitive impairment and neuromuscular dysfunction resulting in profound gait abnormalities. This novel *Rps19* mutant shows behavioural phenotypes resembling that of the human Diamond-Blackfan anaemia syndrome, thus creating the possibility to use this mutant as a unique murine model for studying the molecular basis of ribosomal protein deficiencies.

Introduction

Altered expression of ribosomal proteins (RP) underlies a number of human disorders, most prominent of which are bone marrow failure disorders such as Diamond-Blackfan anaemia (DBA). The core symptom of DBA is severe macrocytic anaemia, resulting from an intrinsic defect in erythroid progenitors. Additional indications, which affect 30–40 % of DBA patients, include growth retardation, skeletal deformation, cognitive deficits, and psychomotor retardation (Ball et al., 1996; Cario et al., 1999; Tentler et al., 2000; Burgess et al., 2014). Mutations in RP are thought to be the primary cause of DBA and can be found in 50–70 % of patients (Gerrard et al., 2013). Affected RPs include *RPS19*, *RPS7*, *RPS10*, *RPS17*, *RPS24*, *RPS26*, *RPL5*, *RPL11* and *RPL35A* (Draptchinskaia et al., 1999; Narla and Ebert, 2010). More than 200 different mutations in DBA-associated genes have been characterized to date (Boria et al., 2010). Among them, mutations in *RPS19* are the most frequent, found in approximately 25 % of DBA patients (Willig et al., 1999; Campagnoli et al., 2004; Gazda et al., 2004).

When present, behavioural symptoms of DBA can be prominent and debilitating (Ball et al., 1996; Gustavsson et al., 1998; Cario et al., 1999; Tentler et al., 2000; Campagnoli et al., 2004; Quarello et al., 2008; Burgess et al., 2014) and are still not well addressed in mouse models of RP deficiency (McGowan and Mason, 2011; Taylor and Zon, 2011; Terzian and Box, 2013; Watkins-Chow et al., 2013). Although mice homozygous for the mutation in *Rps19* were embryonically lethal, heterozygous mice did not present all DBA features. Thus, in contrast to humans, heterozygous mice seem to compensate for *Rps19* haploinsufficiency (Matsson et al., 2004, 2006). We overcame the compensatory effect by the wild-type allele, reported in previous DBA models (Angelini et al., 2007; Gregory et al., 2007), by introducing a hypomorphic mutation into the gene: this mutation (deletion of one amino acid (p.67delR) in RPS19 at the flanking site of α -helix 3) was weak enough to allow homozygous mice to develop and survive, yet strong enough to cause a profound phenotype. While heterozy-

Received April 16, 2016. Accepted May 18, 2016.

Financial support was given to R. S. by IGA (MZ13-UMG; NT15451-3).

Corresponding authors: Radislav Sedláček, Agnieszka Kubik-Zahorodna, Laboratory of Transgenic Models of Diseases, BIOCEV Division, Institute of Molecular Genetics of the ASCR, v. v. i., Videňská 1083, 142 20 Prague 4, Czech Republic. Phone: (+420) 325 873 243 (R. S.); e-mails: radislav.sedlacek@img.cas.cz, agnieszka.kubik-zahorodna@img.cas.cz

Abbreviations: CS – conditioned stimulus, CV – coefficient of variation, DBA – Diamond-Blackfan anaemia, HD – Huntington's disease, ITI – intra-trial interval, PD – Parkinson's disease, RP – ribosomal proteins, SA – spontaneous alternations, TA – total alternations, TE – total arm entries, US – unconditioned stimulus, WT – wild type.

gous (RPS19^{+/67delR}) animals did not express any obvious phenotypes, homozygous mice (RPS19^{67delR/67delR}) presented with growth retardation, white belly spots, macroscopic skeletal deformations, and hydrocephalus.

Here, we report a behavioural characterization of RPS19^{67delR/67delR} mice, which revealed behavioural defects that mirror what has been reported in human DBA case reports (Cario et al., 1999; Tentler et al., 2000; Burgess et al., 2014). These mice exhibited moderate cognitive impairment and neuromuscular dysfunction resulting in profound gait abnormalities. Further systematic and thorough analyses of our mutant could help to elucidate the mechanisms underlying the behavioural phenotype, and could improve understanding of the DBA disease development.

Material and Methods

Mouse model

Heterozygous (RPS19^{+/67delR}) mice on C57Bl/6N background were intercrossed to generate homozygous animals and wild-type (WT) littermates as a control. The mice were weaned between three and four weeks of age and housed in groups of two to six with a 12/12 h light/dark cycle and access to food and water *ad libitum*. RPS19^{67delR/67delR} and WT female mice were investigated at 6–8 weeks of age. Behavioural testing was performed during the light phase. All animal experimentation was performed in accordance with European directive 86/609/EEC and was approved by the Czech Central Commission for Animal Welfare (project No. 40/2015).

Body weight

Animals were weighed at 7th week of age.

Histology

Whole heads from euthanized RPS19^{67delR/67delR} (N = 7) and WT (N = 7) mice were collected and fixed in 4% buffered formaldehyde. After 72 h the heads were de-skinned and placed for one week in Osteosoft® (Merck-Millipore, Darmstadt, Germany) for decalcification. The decalcified samples were trimmed longitudinally and processed in a Leica ASP6025 (Leica Biosystems, Singapore) tissue processor overnight. Sections with 5 µm thickness were obtained from every sample and stained with haematoxylin and eosin in an automated stainer (Ventana Symphony, Ventana Medical Systems, Tucson, AZ). All slides were scanned in an AxioScan.Z1 slide scanner (Carl Zeiss, Goettingen, Germany), viewed and analysed using ZEN2 software (Carl Zeiss).

Neuromuscular assays

Contact righting. The contact righting experiment was performed according to IMPC protocols (<https://www.mousephenotype.org/impress/protocol/186/7>). Contact righting is a motor response by which the animal moves from a supine to prone position, and was

used as a measure of axial coordination. Righting was assessed in a contact righting tube, wherein the mouse was placed on its back and its ability to regain footing was scored as normal (1–5 s) or impaired (> 5 s).

Grip strength measurements. The measurement of grip strength was performed according to the IMPC protocol (<https://www.mousephenotype.org/impress/protocol/186/7>). Forelimb and combined forelimb and hind limb grip strengths were determined using an automated meter (Bioseb, Vitrolles, France). To assess neuromuscular function, the mouse was pulled over a grid; the test was recorded in three trials. To account for potential effects of body mass, all grip strength measurements were normalized against mouse body mass.

Beam-walk. To evaluate fine motor coordination, a beam-walk test was performed as previously described (Yu et al., 2012). Coordination and balance were determined by recording latency to reach an escape box and the number of foot flips during a walk along a wooden beam 100 cm long and 2 cm in diameter. Foot flips were defined as a hind limb slipping from the horizontal surface of the beam. Three trials for each mouse were recorded.

Learning and memory

Fear conditioning. A contextual and cued fear conditioning was performed according to the manufacturer protocol recommendation (Ugo Basile, Gemonio, Italy). The associative learning took place in a cage enclosed within a soundproof cabinet (Ugo Basile). The cage was equipped with a stainless steel rod floor for shock delivery. The acquisition trial started with a 3 min adaptation period, after which mice were presented with two pairings of a conditioned stimulus (CS) (20 s of 4 kHz pure tone at 77 dB) and an unconditioned stimulus (US) (a 1 s, 0.3 mA constant current to the cage floor). The US was presented immediately after the CS. The intra-trial interval (ITI) was 2 min. Mice remained in the chamber for 1 min after the last shock delivery. Animals were tested for contextual memory 24 h after the training. They were reintroduced to the training context and behaviour was recorded for 3 min with no CS or US presentation. Total freezing time was scored for the last 2 min. Delayed cue memory was tested three hours later. Animals were placed in a novel context, with different cage wall pattern and a smooth floor texture. The freezing response to the CS was monitored for 2 min. Freezing, defined as the absence of all movement other than respiration, was detected automatically by ANY-maze software (Stoelting Co., Wood Dale, IL) and reviewed by a trained observer.

Y-maze. The experiment was performed as described in Moran et al. (1995). The Y-maze apparatus consisted of three identical arms. Animals were tested individually, always being placed in the centre of the maze. Light was adjusted to an intensity of 50 lux at the centre of the maze. Animal behaviour was recorded by a digital video camera for a period of 5 min. The percentage of alterna-

tion was calculated automatically by Biobserve software according to the equation $\% SA = (TA \cdot 100) / (TE - 2)$, where SA – spontaneous alternations, TA – total alternations made by the animal, TE – total arm entries.

Rotarod. The protocol was adopted and modified from Paylor et al. (1999). Motor learning was studied using a rod with accelerating speed of rotation (4–40 rpm/5 min, RotaRod, TSE Systems, Bad Homburg, Germany) during five consecutive days. Each day the average latency to falling was determined from three trials with 15 min ITI. The first day analysis served as an evaluation of general balance and motor coordination.

Gait analysis

Treadmill gait assessment was performed using the DigiGait imaging apparatus (DigiGate, Mouse Specifics, Inc., Framingham, MA) as described (Hampton et al., 2011). Mice were placed on a motorized treadmill within an acrylic glass compartment (~25 cm long and ~5 cm wide). Digital video images were acquired at a rate 125 frames per second by a camera positioned below the transparent belt to focus on the ventral view of subjects walking atop of the belt. The treadmill was set at a fixed speed of 15 cm/sec, at which all animals were able to move continuously. The videos were analysed by the DigiGait software, which automatically identifies the paw footprints. Manual adjustments of the image contrast were made to properly distinguish the footprints from the background. The images were then automatically processed by the software to calculate values for multiple gait indices, including stride width, stride length, paw angle, paw area and stance width variability.

Statistical analysis

D'Agostino-Pearson omnibus K2 normality test was used to evaluate the normality of data distribution. The effects of genotype were analysed by Student *t*-test or non-parametric Mann-Whitney test, Fisher's exact test, two-way ANOVA, two-way ANOVA with repeated measurements, and Bonferroni multiple comparisons post-hoc test where appropriate. The α value for all statistical comparisons was 0.05.

Results

RPS19^{67delR/67delR} mice exhibit anatomical malformations and hydrocephalus

RPS19^{67delR/67delR} mice revealed smaller overall size and decreased body mass ($P = 0.0421$; Fig. 1A). In addition, deviations in body posture had been seen in terms of upright tail and head posture (Fig. 1B) and detectable cervical and lumbar curvature lordosis (Fig. 1B, lower panel arrows). Concave appearance of the dorsal facial region was also present (Fig. 1B, lower panel, yellow dashed line). The whole cranial section revealed enlarged lateral ventricles and subarachnoidal space in the mutants, typical features of hydrocephalus (Fig. 2).

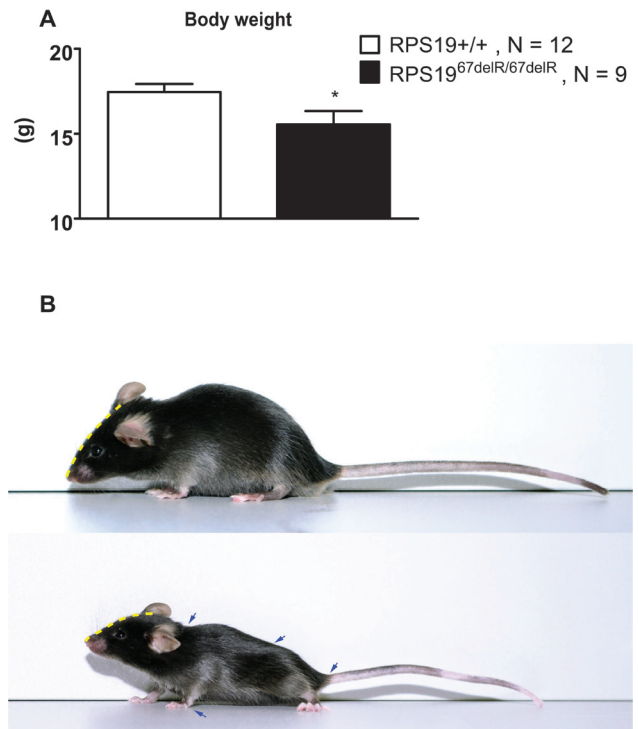


Fig. 1. (A) *RPS19*^{67delR/67delR} mutant mice were smaller than their wild-type littermates according to body weight comparison (Student's *t*-test, $P = 0.0421$). (B) Arrows point at whole body deformations of *Rps19* mutant mouse, yellow lines show abnormal head curvature.

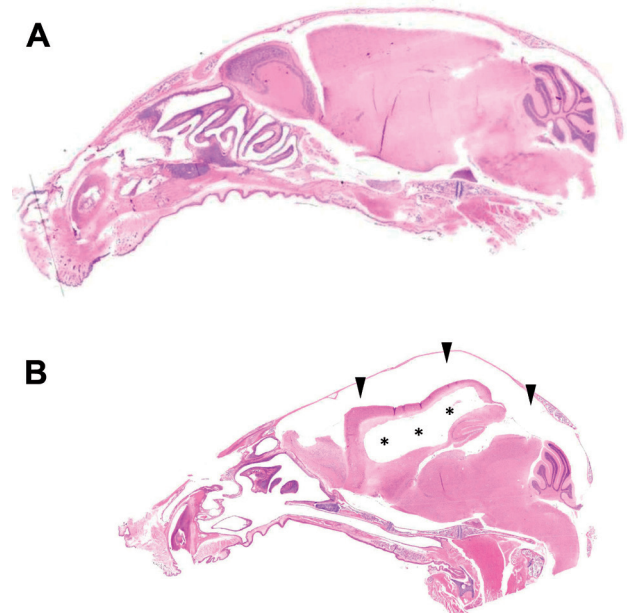


Fig. 2. Whole cranial sections of WT (A) and *RPS19*^{67delR/67delR} mutants (B): the mutants exhibit hydrocephalus manifested by enlarged lateral ventricles (asterisks). Dilated subarachnoid space (arrowheads) is also a feature of *RPS19*^{67delR/67delR} mutants. Haematoxylin and eosin; original magnification: 1.25 \times .

RPS19^{67delR/67delR} mice exhibit neuromuscular defects

To assess selected neuromuscular functions, contact righting, grip strength, and beam-walk tests were employed. *RPS19*^{67delR/67delR} mice exhibited prolonged contact righting compared to their WT littermates (55.56 % versus 8.33 %, Fisher's exact test $P = 0.0231$; Fig. 3A).

Although no differences between genotypes were observed in forelimb grip strength (5.60 ± 0.236 versus 5.84 ± 0.435 , $P = 0.3233$; Fig. 3B), *RPS19*^{67delR/67delR} mice demonstrated weaker grip for combined forelimb and hind limb measurements than their WT littermates (7.99 ± 0.583 versus 9.59 ± 0.455 , $P = 0.0418$; Fig. 3C).

To measure balance and coordination, the beam-walk test was performed. Both mutant and WT mice reached an escape box within a similar time period (9.04 ± 0.715 versus 7.81 ± 0.431 , $P = 0.187$; Fig. 3D); however, the *RPS19*^{67delR/67delR} mice displayed a considerable increase of foot flips comparing to WT mice (4.04 ± 1.004 versus

0.47 ± 0.119 , $P = 0.0006$; Fig. 3E). The results of all three assays indicate a neuromuscular impairment of homozygous mice.

Learning and memory deficits in *RPS19*^{67delR/67delR} mice

In the fear conditioning, both wild-type and mutant mice froze significantly more during the probe trials compared to their baseline recordings from the training day, indicating successful learning in both genotypes ($F_{2,32} = 24.54$, $P < 0.0001$; Fig. 4). However, homozygous *RPS19*^{67delR/67delR} mice froze consistently less than WT animals (genotype effect $F_{1,16} = 6.8$, $P = 0.019$), showing that *RPS19*^{67delR/67delR} mice exhibit a deficit in associative learning. The experiment in Y-maze did not reveal any differences either in percent of spontaneous alternation or total track length, suggesting no alternations in working memory and general activity, respectively ($P = 0.7218$ and $P = 0.1886$; Fig. 5A,B).

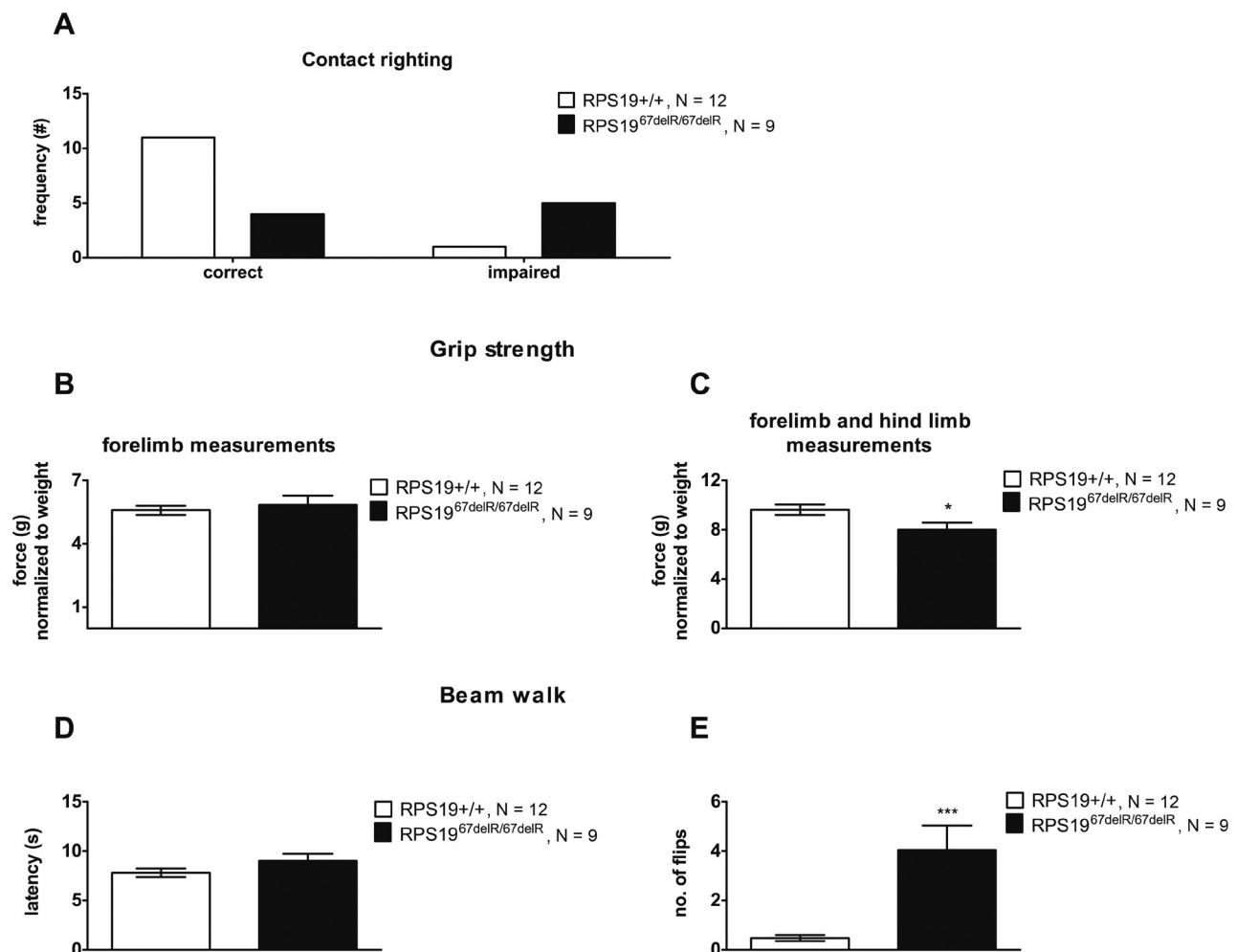


Fig. 3. (A) Contingency analysis of normal and prolonged contact righting distribution (Fisher's exact test, $P = 0.0231$) reveals a defect in righting reflex in *Rps19* mutant mice. (B, C) Grip strength was normalized against body weight. (B): comparison of forelimb strength (Mann-Whitney test, $P = 0.3028$), (C): comparison of combined forelimb and hind limb strength (Student's t -test, $P = 0.0302$). (D, E) Sensorimotor evaluation on beam walk. (D): latency to reach an escape box (Mann-Whitney test, $P = 0.187$), (E): number of foot flips (Student's t -test, $P = 0.0006$). Data are presented as mean with SEM.

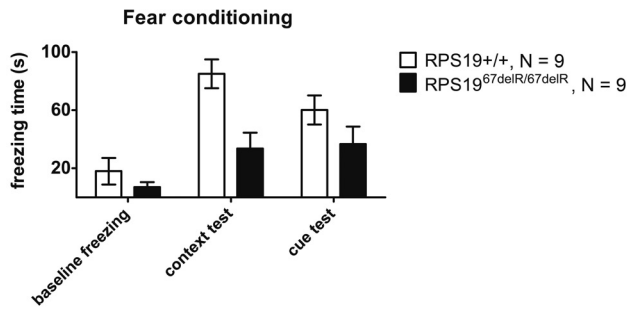


Fig. 4. Contextual and delayed cued fear conditioning. Total freezing time measured in the last 2 min of adaptation period in acquisition trial, last 2 min of contextual test, and 2 min after cue tone presentation in delayed cue test. Data was analysed by two-way ANOVA with repeated measurements (trial effect: $F_{2,32} = 24.54$, $P < 0.0001$; genotype effect: $F_{1,16} = 6.8$, $P = 0.019$). Data are presented as mean with SEM.

The performance on rotarod was comparable between mutants and their WT littermates ($F_{1,19} = 0.9$, $P = 0.3552$; Fig. 6A). Also, motor learning on the rotarod did not show significant differences between WT and mutant mice ($F_{1,19} = 3.06$, $P = 0.0963$; Fig. 6B).

Altered gait dynamics in *RPS19*^{67delR/67delR} mice

Gait analysis revealed differences in temporal and spatial indices (Table 1) correlating with body size. As the *RPS19*^{67delR/67delR} mice were smaller than their WT littermates (Fig. 1A, B), they had to adjust their movement to the belt speed. As a result, the smaller *RPS19*^{67delR/67delR} mice had shorter swing, propulsion, stance, and stride duration; shorter stride length and higher stride frequency. Figure 7 displays additional abnormalities observed in *RPS19*^{67delR/67delR} mice in gait parameters whose origin

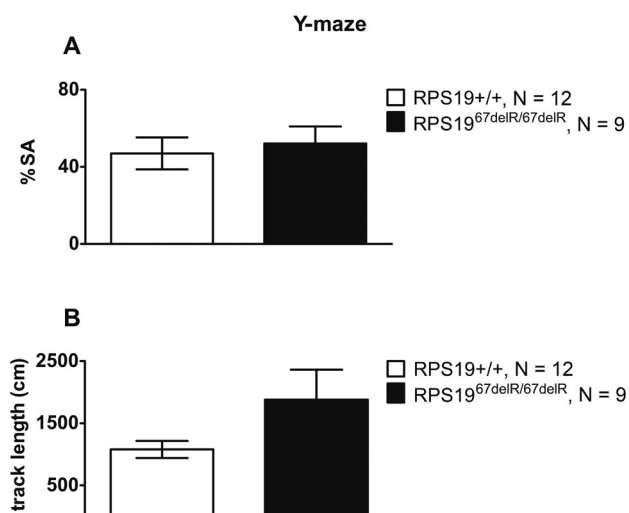


Fig. 5. Working memory tested as spontaneous alternation behaviour in Y-maze and general activity evaluated by total distance travelled during a test. (A) There were no significant genotype differences in % of spontaneous alternations (Student's *t*-test, $P = 0.7218$) (B) neither in total distance travelled (Student's *t*-test, $P = 0.1886$).

cannot be ascribed only to the animal size. *RPS19*^{67delR/67delR} mice had more open forepaw angle (pronation) but showed tendency for less open hind paw placement angle (Fig. 7A, interaction effect: $F_{1,38} = 15.26$, $P = 0.0002$). Step-to-step variability in stance width of *RPS19*^{67delR/67delR} mice was considerably increased compared to WT animals (Fig. 7B, genotype effect: $F_{1,38} = 13.88$, $P = 0.0006$). In mice, higher variability in stance width is associated with falls (Lin et al., 2001; Amende et al., 2005). A measure of stride-to-stride variability is expressed in the coefficient of variation (CV), and this was significantly higher in forepaws of *RPS19*^{67delR/67delR} mice (Fig. 7C, genotype effect: $F_{1,38} = 13.71$, $P = 0.0007$). The CV of forepaw stance width of *RPS19*^{67delR/67delR} mice was 36.12%, with the normal CV range ranging between ~15–20% (Amende et al., 2005). A significant interaction effect of paw area at the peak stance ($F_{1,38} = 12.54$, $P = 0.0007$) indicates that *RPS19*^{67delR/67delR} mice had a smaller hind paw area with preserved forepaw area (Fig. 7D), which could suggest a shifted centre of gravity. These findings are supported by the anatomical spinal aberration observed in *RPS19*^{67delR/67delR} mice (Fig. 1B). Both maximum and minimum rate of hind paw area change during contact with the belt was attenuated in *RPS19*^{67delR/67delR} mice (Fig. 7E, F, genotype effect for max dA/dt: $F_{1,38} = 4.53$, $P = 0.0364$, and for min dA/dt

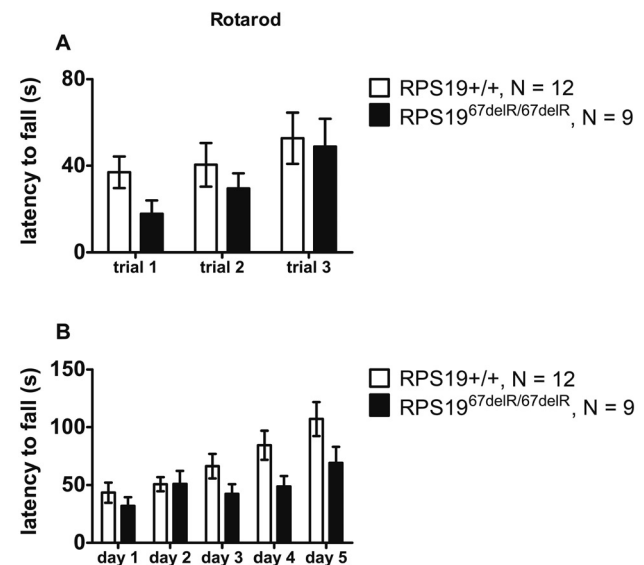


Fig. 6. (A) Balance and movement coordination on rotarod, three trials with ITI 15 min. Latency to falling from accelerating rod (4–40 rpm/5 min) was measured. No differences between mutants and normal mice were detected. Data was analysed by two-way ANOVA with repeated measurements (trial effect: $F_{2,38} = 0.78$, $P = 0.464$; genotype effect: $F_{1,19} = 0.9$, $P = 0.3552$). (B) Motor learning analysed on rotarod on 5 consecutive days. Latency to falling from accelerating rod (4–40 rpm/5 min) was measured. No significant difference was reported between mutant and normal mice. Data was analysed by two-way ANOVA with repeated measurements (day effect: $F_{4,76} = 13.53$, $P < 0.0001$; genotype effect: $F_{1,19} = 3.06$, $P = 0.0963$).

Table 1. Reported significant differences in listed gait parameters are due to the reduced size of *RPS19^{67delR/67delR}* mutant mice.

		RPS19 ^{+/+}	RPS19 ^{67delR/67delR}	P value
		mean ± SE	mean ± SE	
swing duration	forelimbs	0.1250 ms ± 0.0054	0.0990 ms ± 0.0947	< 0.0001
	hind limbs	0.1140 ms ± 0.0044	0.0950 ms ± 0.0063	
propulsion duration	forelimbs	0.1710 ms ± 0.0060	0.1480 ms ± 0.0066	< 0.0001
	hind limbs	0.1820 ms ± 0.0065	0.1490 ms ± 0.0065	
stance duration	forelimbs	0.2190 ms ± 0.0059	0.1990 ms ± 0.0037	< 0.0001
	hind limbs	0.2330 ms ± 0.0067	0.1990 ms ± 0.0048	
stride duration	forelimbs	0.3450 ms ± 0.0093	0.2990 ms ± 0.0069	< 0.0001
	hind limbs	0.3470 ms ± 0.0098	0.2930 ms ± 0.0087	
stride length	forelimbs	5.20 cm ± 0.14	4.50 cm ± 0.11	< 0.0001
	hind limbs	5.20 cm ± 0.15	4.40 cm ± 0.13	
stride frequency	forelimbs	2.970 ± 0.078	3.400 ± 0.081	< 0.0001
	hind limbs	2.970 ± 0.087	3.510 ± 0.108	
midline distance	forelimbs	2.970 cm ± 0.085	2.520 cm ± 0.117	< 0.0001
	hind limbs	1.290 cm ± 0.075	0.970 cm ± 0.136	

Gait analysis

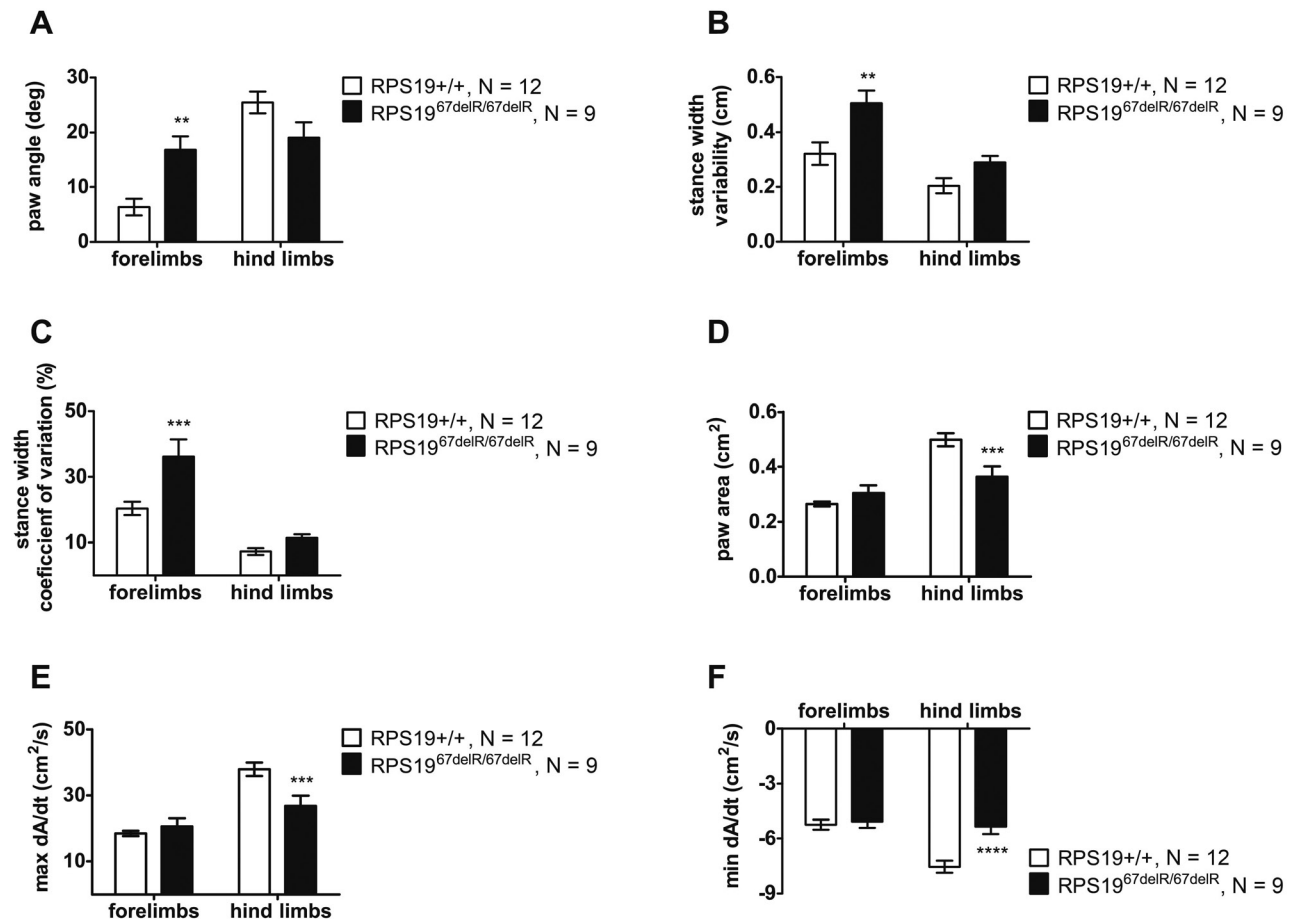


Fig. 7. Analysis of gait dynamics. (A) Paw angle measurement, (B) stance width variability and (C) stance width variability coefficient of variation, (D) paw area evaluation, (E) maximal paw area change at initiation of stance, (F) minimal paw area change at the end of stance. Comparisons were made using two-way ANOVA. Bonferroni multiple comparisons were used as a post-hoc test (**and *** indicates $P < 0.01$ and $P < 0.001$, respectively). Data are presented as mean with SEM.

$F_{1,38} = 12.41$, $P = 0.0007$). These parameters describe how quickly an animal loads and unloads its limbs during the initial and later period of stance (Bartley et al., 2016). The obtained results suggest weaker muscle strength of the hind limbs and are consistent with the grip strength measurement results described earlier.

Discussion

In this study, we investigated the impact of RPS19 single amino residue mutation on behavioural phenotypes, associated with anatomical and morphological changes. Our mutant mice exhibit compromised cognitive abilities and neuromuscular defects that affect the postural reflex (contact righting), fine motor coordination, and muscular strength. Impairment in contact righting may indicate malfunction of proprioceptive-tactile responses or vestibular system (Pellis et al., 1989; Pellis and Pellis, 1994), although higher brain structures, like the cerebellum and thalamus, as well as axial musculature are also involved in postural reflexes (Martens et al., 1996). RPS19 mutant mice have a visible skull bump often reported in mice with hydrocephalus (Zhang et al., 2006; Lee et al., 2012). Skull deformation could affect normal brain development and later on, its function. Indeed, preliminary histopathological examination revealed expansion of ventricular and subarachnoid spaces with contracted brain. Similarly, enlarged ventricles and thinner cortex were reported in RPS7 mutants (Watkins-Chow et al., 2013).

Although initial performance of RPS19^{67delR/67delR} mice on rotarod and their overall activity, evaluated in the Y-maze test, did not differ from their WT littermates, the mutant mice made considerable more foot flips in the beam-walk test. An increased number of foot flips is consistent with higher stance width variability, as the stance width variability associates with fall counts (Lin et al., 2001; Amende et al., 2005). This behaviour was also observed in animal models of Parkinson's (PD) and Huntington's (HD) diseases, where motor control deficit is a major symptom (Borlongan et al., 1997; Amende et al., 2005). Even though the pathology of PD and HD involves different parts of the basal ganglia, postural instability is a common feature to both diseases. Strong brain deformation may be a reason of insufficient control of movement by higher brain structures. An increase in the frequency of foot flips and higher stance width variability may also be related to the attenuated hind limb muscle strength observed in RPS19^{67delR/67delR} mice.

Weaker hind limbs can also result in altered dynamics of paw rise and placement during the stance period (Vinsant et al., 2013a, b; Bartley et al., 2016). General activity and gross motor skills were not affected, although a fine movement coordination defect was reflected in gait deviations such as altered paw placement angle and larger hind paw area. A larger contact area of hind paw with sustained area of forepaws suggests a potential shift in the centre of gravity, and together with altered paw placement positioning, reflects changes in

the support base. These changes may be compensatory to muscular and vestibular defects and may act to help maintain posture and balance (Vinsant et al., 2013a, b; Liu et al., 2015; Rinalduzzi et al., 2015). It is likely that in addition to an abnormally developed brain and weaker hind limbs, the skeletal deformations in RPS19^{67delR/67delR} mice also contribute to the defects in mouse gait. Normal performance on rotarod suggests proper cerebellum function in the RPS19 mutants. However, dysfunctions in other areas such as the motor cortex, striatum, or nigrostriatal pathway may be responsible for abnormalities in precise motor coordination described in the previous paragraph. Further investigation will be necessary to elucidate the precise neuronal basis of the observed behavioural phenotype.

Motor delay and intellectual disability are the most often described behavioural symptoms in DBA patients (Gustavsson et al., 1998; Tentler et al., 2000; Campagnoli et al., 2004; Quarello et al., 2008). The RPS19^{67delR/67delR} mice show moderate impairment of associative memory. Memory deficit is profound in contextual testing, indicating hippocampal dysfunction. It appears to be limited to long-term memory, as working memory, tested in the Y-maze, was intact. These results suggest that complex forms of associative learning and memory may be impaired in RPS19 mutant mice. We also observed an obvious tendency towards poorer learning on rotarod tested during five consecutive days. In general, the results of associative memory and motor learning tests may suggest a general deficit in learning processes.

In conclusion, one amino acid deletion in *Rps19* produced a profound behavioural phenotype related to neuromuscular and cognitive functions. Neuromuscular defects accompanied by additional body and brain alterations can be direct causes of altered gait in mutant mice. Cognitive impairment in mutants could be a consequence of observed brain deformation, although more detailed analysis will be needed to explain the neuronal basis of the deficit. Similar behavioural and anatomical alterations have also been described for DBA patients with reported depletions or alterations of RPS19, including motor delay, intellectual disability, hypotonia, macrocephaly, psychomotor retardation, skeletal malformations, and craniofacial abnormalities (Gustavsson et al., 1998; Tentler et al., 2000; Campagnoli et al., 2004; Quarello et al., 2008). Up-to-date, only one murine model of DBA-associated genes (*Rps7* mutation) described a behavioural phenotype in the face of severe neuroanatomical and histological changes of the mutant's central nervous system (Watkins-Chow et al., 2013). RPS19^{67delR/67delR} mutant mice appear to be a useful model recapitulating traits found in DBA patients and could be further employed to reveal the role of RPS19 in the context of DBA development.

Acknowledgment

We thank Cynthia Drachovsky for outstanding technical assistance in behavioural tests. We are also grateful to Trevor Epp for critical reading of the manuscript.

References

- Amende, I., Kale, A., McCue, S., Glazier, S., Morgan, J. P., Hampton, T. G. (2005) Gait dynamics in mouse models of Parkinson's disease and Huntington's disease. *J. Neuroeng. Rehabil.* **2**, 20.
- Angelini, M., Cannata, S., Mercaldo, V., Gibello, L., Santoro, C., Dianzani, I., Loreni, F. (2007) Missense mutations associated with Diamond-Blackfan anemia affect the assembly of ribosomal protein S19 into the ribosome. *Hum. Mol. Genet.* **16**, 1720-1727.
- Ball, S. E., McGuckin, C. P., Jenkins, G., Gordon-Smith, E. C. (1996) Diamond-Blackfan anaemia in the U.K.: analysis of 80 cases from a 20-year birth cohort. *Br. J. Haematol.* **94**, 645-653.
- Bartley, J. M., Pan, S. J., Keilich, S. R., Hopkins, J. W., Al-Naggar, I. M., Kuchel, G. A., Haynes, L. (2016) Aging augments the impact of influenza respiratory tract infection on mobility impairments, muscle-localized inflammation, and muscle atrophy. *Aging (Albany NY)*, Epub ahead of print.
- Boria, I., Garelli, E., Gazda, H. T., Aspesi, A., Quarello, P., Pavesi, E., Ferrante, D., Meerpohl, J. J., Kartal, M., Da Costa, L., Proust, A., Leblanc, T., Simansour, M., Dahl, N., Fröjmark, A. S., Pospisilova, D., Cmejla, R., Beggs, A. H., Sheen, M. R., Landowski, M., Buros, C. M., Clinton, C. M., Dobson, L. J., Vlachos, A., Atsidaftos, E., Lipton, J. M., Ellis, S. R., Ramenghi, U., Dianzani, I. (2010) The ribosomal basis of Diamond-Blackfan anemia: mutation and database update. *Hum. Mutat.* **31**, 1269-1279.
- Borlongan, C. V., Koutouzis, T. K., Sanberg, P. R. (1997) 3-Nitropropionic acid animal model and Huntington's disease. *Neurosci. Biobehav. Rev.* **21**, 289-293.
- Burgess, T., Brown, N. J., Stark, Z., Bruno, D. L., Oertel, R., Chong, B., Calabro, V., Kornberg, A., Sanderson, C., Kelly, J., Howell, K. B., Savarirayan, R., Hinds, R., Greenway, A., Slater, H. R., White, S. M. (2014) Characterization of core clinical phenotypes associated with recurrent proximal 15q25.2 microdeletions. *Am. J. Med. Genet. A* **164A**, 77-86.
- Campagnoli, M. F., Garelli, E., Quarello, P., Carando, A., Varotto, S., Nobili, B., Longoni, D., Pecile, V., Zecca, M., Dufour, C., Ramenghi, U., Dianzan, I. (2004) Molecular basis of Diamond-Blackfan anemia: new findings from the Italian registry and a review of the literature. *Haematologica* **89**, 480-489.
- Cario, H., Bode, H., Gustavsson, P., Dahl, N., Kohne, E. (1999) A microdeletion syndrome due to a 3-Mb deletion on 19q13.2 – Diamond-Blackfan anemia associated with macrocephaly, hypotonia, and psychomotor retardation. *Clin. Genet.* **55**, 487-492.
- Draptchinskaia, N., Gustavsson, P., Andersson, B., Pettersson, M., Willig, T.N., Dianzani, I., Ball, S., Tchernia, G., Klar, J., Matsson, H., Tentler, D., Mohandas, N., Carlsson, B., Dahl, N. (1999) The gene encoding ribosomal protein S19 is mutated in Diamond-Blackfan anaemia. *Nat. Genet.* **21**, 169-175.
- Gazda, H. T., Zhong, R., Long, L., Niewiadomska, E., Lipton, J. M., Ploszynska, A., Zaucha, J. M., Vlachos, A., Atsidaftos, E., Viskochil, D. H., Niemeyer, C. M., Meerpohl, J. J., Rokicka-Milewska, R., Pospisilova, D., Wiktor-Jedrzejczak, W., Nathan, D. G., Beggs, A. H., Sieff, C. A. (2004) RNA and protein evidence for haplo-insufficiency in Diamond-Blackfan anaemia patients with RPS19 mutations. *Br. J. Haematol.* **127**, 105-113.
- Gerrard, G., Valganon, M., Foong, H. E., Kasperaviciute, D., Iskander, D., Game, L., Muller, M., Aitman, T. J., Roberts, I., de la Fuente, J., Foroni, L., Karadimitris, A. (2013) Target enrichment and high-throughput sequencing of 80 ribosomal protein genes to identify mutations associated with Diamond-Blackfan anaemia. *Br. J. Haematol.* **162**, 530-536.
- Gregory, L. A., Aguisa-Toure, A. H., Pinaud, N., Legrand, P., Gleizes, P. E., Fribourg, S. (2007) Molecular basis of Diamond-Blackfan anemia: structure and function analysis of RPS19. *Nucleic Acids Res.* **35**, 5913-5921.
- Gustavsson, P., Garelli, E., Draptchinskaia, N., Ball, S., Willig, T. N., Tentler, D., Dianzani, I., Punnett, H. H., Shafer, F. E., Cario, H., Ramenghi, U., Glomstein, A., Pfeiffer, R. A., Goringe, A., Olivieri, N. F., Smibert, E., Tchernia, G., Elinder, G., Dahl, N. (1998) Identification of microdeletions spanning the Diamond-Blackfan anemia locus on 19q13 and evidence for genetic heterogeneity. *Am. J. Hum. Genet.* **63**, 1388-1395.
- Hampton, T. G., Kale, A., Amende, I., Tang, W., McCue, S., Bhagavan, H. N., VanDongen, C. G. (2011) Gait disturbances in dystrophic hamsters. *J. Biomed. Biotechnol.* **2011**, 235354.
- Lee, K., Tan, J., Morris, M. B., Rizzoti, K., Hughes, J., Cheah, P. S., Felquer, F., Liu, X., Piltz, S., Lovell-Badge, R., Thomas, P. Q. (2012) Congenital hydrocephalus and abnormal subcommissural organ development in Sox3 transgenic mice. *PLoS One* **7**, e29041.
- Lin, C. H., Tallaksen-Greene, S., Chien, W. M., Cearley, J. A., Jackson, W. S., Crouse, A. B., Ren, S., Li, X. J., Albin, R. L., Detloff, P. J. (2001) Neurological abnormalities in a knock-in mouse model of Huntington's disease. *Hum. Mol. Genet.* **10**, 137-144.
- Liu, Y. B., Tewari, A., Salameh, J., Arystarkhova, E., Hampton, T. G., Brashear, A., Ozelius, L. J., Khodakhah, K., Sweadner, K. J. (2015) A dystonia-like movement disorder with brain and spinal neuronal defects is caused by mutation of the mouse laminin β 1 subunit, Lamb1. *eLife* **4**.
- Martens, D. J., Whishaw, I. Q., Miklyaeva, E. I., Pellis, S. M. (1996) Spatio-temporal impairments in limb and body movements during righting in an hemiparkinsonian rat analogue: relevance to axial apraxia in humans. *Brain Res.* **733**, 253-262.
- Matsson, H., Davey, E. J., Draptchinskaia, N., Hamaguchi, I., Ooka, A., Leveen, P., Forsberg, E., Karlsson, S., Dahl, N. (2004) Targeted disruption of the ribosomal protein S19 gene is lethal prior to implantation. *Mol. Cell. Biol.* **24**, 4032-4037.
- Matsson, H., Davey, E. J., Fröjmark, A. S., Miyake, K., Ut-sugisawa, T., Flygare, J., Zahou, E., Byman, I., Landin, B., Ronquist, G., Karlsson, S., Dahl, N. (2006) Erythropoiesis in the Rps19 disrupted mouse: analysis of erythropoietin response and biochemical markers for Diamond-Blackfan anemia. *Blood Cells Mol. Dis.* **36**, 259-264.
- McGowan, K. A., Mason, P. J. (2011) Animal models of Diamond Blackfan anemia. *Semin. Hematol.* **48**, 106-116.

- Moran, P. M., Higgins, L. S., Cordell, B., Moser, P. C. (1995) Age-related learning deficits in transgenic mice expressing the 751-amino acid isoform of human β -amyloid precursor protein. *Proc. Natl. Acad. Sci. USA* **92**, 5341-5345.
- Narla, A., Ebert, B. L. (2010) Ribosomopathies: human disorders of ribosome dysfunction. *Blood* **115**, 3196-3205.
- Paylor, R., Hirotsune, S., Gambello, M. J., Yuva-Paylor, L., Crawley, J. N., Wynshaw-Boris, A. (1999) Impaired learning and motor behavior in heterozygous *Pafah1b1* (*Lis1*) mutant mice. *Learn. Mem.* **6**, 521-537.
- Pellis, S. M., Pellis, V. C., Chen, Y. C., Barzci, S., Teitelbaum, P. (1989) Recovery from axial apraxia in the lateral hypothalamic labyrinthectomized rat reveals three elements of contact-righting: cephalocaudal dominance, axial rotation, and distal limb action. *Behav. Brain Res.* **35**, 241-251.
- Pellis, S. M., Pellis, V. C. (1994) Development of righting when falling from a bipedal standing posture: evidence for the dissociation of dynamic and static righting reflexes in rats. *Physiol. Behav.* **56**, 659-663.
- Quarello, P., Garelli, E., Brusco, A., Carando, A., Pappi, P., Barberis, M., Coletti, V., Campagnoli, M. F., Dianzani, I., Ramenghi, U. (2008) Multiplex ligation-dependent probe amplification enhances molecular diagnosis of Diamond-Blackfan anemia due to RPS19 deficiency. *Haematologica* **93**, 1748-1750.
- Rinalduzzi, S., Trompetto, C., Marinelli, L., Alibardi, A., Misori, P., Fattapposta, F., Pierelli, F., Curra, A. (2015) Balance dysfunction in Parkinson's disease. *Biomed. Res. Int.* **2015**, 434683.
- Taylor, A. M., Zon, L. I. (2011) Modeling Diamond Blackfan anemia in the zebrafish. *Semin. Hematol.* **48**, 81-88.
- Tentler, D., Gustavsson, P., Elinder, G., Eklof, O., Gordon, L., Mandel, A., Dahl, N. (2000) A microdeletion in 19q13.2 associated with mental retardation, skeletal malformations, and Diamond-Blackfan anaemia suggests a novel contiguous gene syndrome. *J. Med. Genet.* **37**, 128-131.
- Terzian, T., Box, N. (2013) Genetics of ribosomal proteins: "curiouser and curiouser". *PLoS Genet.* **9**, e1003300.
- Vinsant, S., Mansfield, C., Jimenez-Moreno, R., Del Gaizo Moore, V., Yoshikawa, M., Hampton, T. G., Prevet, D., Caress, J., Oppenheim, R. W., Milligan, C. (2013a) Characterization of early pathogenesis in the SOD1(G93A) mouse model of ALS: part I, background and methods. *Brain Behav.* **3**, 335-350.
- Vinsant, S., Mansfield, C., Jimenez-Moreno, R., Del Gaizo Moore, V., Yoshikawa, M., Hampton, T. G., Prevet, D., Caress, J., Oppenheim, R. W., Milligan, C. (2013b) Characterization of early pathogenesis in the SOD1(G93A) mouse model of ALS: part II, results and discussion. *Brain Behav.* **3**, 431-457.
- Watkins-Chow, D. E., Cooke, J., Pidsley, R., Edwards, A., Slotkin, R., Leeds, K. E., Mullen, R., Baxter, L. L., Campbell, T. G., Salzer, M. C., Biondini, L., Gibney, G., Phan Dinh Tuy, F., Chelly, J., Morris, H. D., Riegler, J., Lythgoe, M. F., Arkell, R. M., Loreni, F., Flint, J., Pavan, W. J., Keays, D. A. (2013) Mutation of the diamond-blackfan anemia gene *Rps7* in mouse results in morphological and neuroanatomical phenotypes. *PLoS Genet.* **9**, e1003094.
- Willig, T. N., Draptchinskaia, N., Dianzani, I., Ball, S., Niemeyer, C., Ramenghi, U., Orfali, K., Gustavsson, P., Garelli, E., Brusco, A., Tiemann, C., Pérignon, J. L., Bouchier, C., Cicchiello, L., Dahl, N., Mohandas, N., Tchernia, G. (1999) Mutations in ribosomal protein S19 gene and Diamond Blackfan anemia: wide variations in phenotypic expression. *Blood* **94**, 4294-4306.
- Yu, F., Wang, Z., Tchanchou, F., Chiu, C. T., Zhang, Y., Chuang, D. M. (2012) Lithium ameliorates neurodegeneration, suppresses neuroinflammation, and improves behavioral performance in a mouse model of traumatic brain injury. *J. Neurotrauma* **29**, 362-374.
- Zhang, W., Yi, M. J., Chen, X., Cole, F., Krauss, R. S., Kang, J. S. (2006) Cortical thinning and hydrocephalus in mice lacking the immunoglobulin superfamily member CDO. *Mol. Cell. Biol.* **26**, 3764-3772.